

1 **Genome-wide Association Study Reveals that *PvGUX1_1* is Associated with Pod**
2 **Stringlessness in Snap Bean (*Phaseolus vulgaris* L.)**

3

4 **Zhiyuan Liu[†], Shuo Gao[†], Helong Zhang, Zhaosheng Xu, Wei Qian***

5

6 Institute of Vegetables and Flowers, Chinese Academy of Agricultural Sciences,
7 Beijing, China

8

9 [†] These authors contributed equally to this work.

10 *** Correspondence:**

11 Wei Qian, qianwei@caas.cn

12

13

14

15

16

17

18

19

20

21

22

23

24

25

26

27

28

29

30

31

32

33

34

35

36

37

38

39

40

41

42

43 **Abstract**

44 The suture strings is a particularly important pod trait that determines the quality
45 and texture of snap bean (*Phaseolus vulgaris* L.). The *St* locus on chromosome 2 has
46 been described as a major locus associated with suture strings. However, the gene and
47 genetic basis underlying this locus remain unknown. Here, we investigated the suture
48 strings of 138 snap bean accessions across two years. A total of 3.66 million
49 single-nucleotide polymorphisms (SNPs) were obtained by deep resequencing. Based
50 on these SNPs, we identified a strong association signal on Chr02 and a promising
51 candidate gene, *PvGUXI_1*. Further analysis revealed that the 2-bp deletion in exon
52 of *PvGUXI_1* was significantly associated with stringlessness. Comparative mapping
53 indicated that *PvGUXI_1* was a domesticated locus and diverged from *PvGUXI_2*
54 during an early stage. Our study provides important insights into the genetic
55 mechanism of suture string formation and useful information for snap bean
56 improvement.

57

58 **Keywords** : Snap bean, Genome-wide association study, Candidate gene, Pod
59 stringlessness, Syntenic analysis

60

61 **Introduction**

62 Snap bean (*Phaseolus vulgaris* L.) is a type of common bean that is harvested before
63 the seeds mature and eaten as a vegetable. Immature snap bean pods are succulent and
64 rich in protein, carbohydrates, vitamin C, vitamin K, and carotenoids (Myers and
65 Kmiecik, 2017). Therefore, the whole pods of snap bean are used for cooking, or
66 preserved for freezing and canning (Hagerty et al., 2016). The snap bean is mainly
67 consumed in North America, Europe, the Middle East, Africa, and Asia. In recent year,
68 China has become the first producer of snap beans in the world (Zhang et al., 2008).

69 Improving pod quality is a major objective for snap bean breeding. Some pod
70 characteristics, including pod length, pod shape, spur length, and the absence or
71 presence of suture strings, have made the snap bean more palatable than the dry bean
72 (another type of common bean in which the mature seed is consumed). A snap bean
73 with the straight, smooth pod, and lacks suture strings is preferred in the fresh market.
74 The fiber string along the suture is usually discarded before being eaten. Thus, the
75 absence of suture strings is more popular with consumers and facilitates the
76 commercial processing of snap bean.

77 Reducing suture strings in snap bean is crucial, and the key to this effort lies in
78 understanding the genetic basis of the formation and development of suture string.
79 The inheritance analysis of suture strings revealed that stringlessness was governed by
80 a dominant gene, *St*, in common bean (Prakken, 1934). Quantitative trait locus (QTL)

81 analysis located the *St* gene on chromosome Pv02 in common bean (Koinange et al.,
82 1996). Working with a recombinant inbred line derived from dry bean and snap bean,
83 a strong QTL, PST2.2, was also found on Pv02, accounting for 32% of total genetic
84 variation in a recombinant inbred line (Hagerty et al., 2016). As the reduction of
85 suture strings and pod wall fibers commonly lead to pod indehiscence in common
86 bean, the indehiscent gene *PvIND* (a homolog of the Arabidopsis INDEHISCENT
87 gene, *IND*) mapped near the *St* locus was predicted to be the *St* gene. However, there
88 was incomplete co-segregation between *PvIND* and the *St* locus and a lack of
89 polymorphisms with dehiscent/indehiscent phenotypes, suggesting that *PvIND* was
90 not the gene *St* (Gioia et al., 2012). Recently, a single QTL, qPD5.1-PV, determining
91 pod indehiscence was identified on chromosome Pv05 (Rau et al., 2019). In the
92 attempt to identify the candidate gene underlying the QTL, a BC4/F4 introgression
93 line population was used to narrow down the QTL in a 22.5 kb region and identified
94 *PvMYB26* was the best candidate gene based on mapping and gene expression pattern
95 (Di Vittori et al., 2020). In addition, several genes or QTLs were also discovered to be
96 associated with pod dehiscence, such as *PvPdh1* on chromosome Pv03, QTLs on
97 Pv08, Pv05 and Pv09 (Parker et al., 2020).

98 The first common bean reference genome was published in 2014 (Schmutz et al.,
99 2014), which made it possible to use different strategies to identify candidate genes
100 and molecular markers for important agronomic traits. Genome-wide association
101 study (GWAS) is an approach based on using the numbers of single-nucleotide
102 polymorphisms (SNPs) to test the association of desired traits. Due to the reduced cost
103 of resequencing, and the repeatability of SNPs in the genome, GWAS has been
104 performed using various landraces and breeding lines in common bean. These studies
105 have focused on grain yield (Kamfwa et al., 2015; Moghaddam et al., 2016; Wu et al.,
106 2020), flowering time (Raggi et al., 2019), resistance to disease (Wu et al., 2017),
107 resistance to pod shattering (Parker et al., 2020), grain mineral content (Delfini et al.,
108 2021), drought resistance (Wu et al., 2021), and abiotic stress (Soltani et al., 2018).
109 However, few studies have focused on specific traits in snap bean (Myers et al., 2019).
110 Pod stringlessness is particularly crucial in snap bean. Therefore, the objective of this
111 study was to identify the candidate gene associated with this trait as a basis for further
112 improving the quality of snap bean.

113

114 **Materials and Methods**

115

116 **Plant material and resequencing**

117 One hundred and thirty-eight snap bean accessions collected from the Institute of
118 Vegetables and Flowers at the Chinese Academy of Agriculture Sciences (CAAS),

119 including landraces, elite lines, and breeding lines, were grown between March and
120 June in 2019 and 2020 (Supplementary Table 1). These seeds were grown in mixed
121 nutrient soil at a greenhouse in Beijing(40° N, 116° E). The plants were watered using
122 automatic drip irrigation every 2-3 days throughout entire growth period. The field
123 away from plant was covered with a mulching plastic sheet to reduce the weed.

124 Young leaves at the unifoliate growth stage from each accession were collected,
125 flash-frozen in liquid nitrogen and stored in an ultra-low-temperature freezer. Genomic
126 DNAs were isolated for each genotype using Plant Genomic DNA kit (Tiangen,
127 Beijing) following to the instructions. The integrity of gDNA was determined on 1%
128 agarose gels. The concentration and quality of gDNA were measured using a
129 NanoDrop2000 Spectrophotometer (Thermo Fisher Scientific). The DNA library were
130 constructed according to the manufacturer's instructions for the TruSeq nano DNA kit
131 (Illumina). The libraries were genotyped using an Illumina HiSeq 2000 (125PE)
132 sequencer at the facilities of Berry Genomics Co. Ltd, Beijing, China, as described by
133 Wu et al. (2020).

134 **Measurement of pod sutures**

135 At the green mature stage, 10 fresh pods from different plants of each accession were
136 randomly chosen to measure the pod suture strings. The 10 pods from 10 individuals
137 served as technical replications. The strings were evaluated as both a qualitative trait
138 and a quantitative trait. As a qualitative trait, the pod strings were scaled 0–1 (0 = no
139 suture strings, 1 = presence of suture strings). As a quantitative trait, the ratio (string
140 length/pod length) of each pod was measured. The average ratio value of 10 pods and
141 the scale rating of pods were both used for GWAS analysis.

142 **Expression analysis of *PvGUX1_1***

143 Three stages (T1 for pod elongation, T2 for pod development, and T3 for pod
144 maturity) of R02 (non-suture pod) and R05 (suture pod) were sampled. The total RNA
145 of the three stages of pods in suture pods and non-suture pods was extracted and
146 converted to cDNA using a Reverse Transcription Kit (TransGen Biotech, Beijing,
147 China) according to the manufacturer's instructions. Quantitative real-time PCR was
148 performed with SYBR Green (Vazyme Biotech, Nanjing, China), and the data
149 collection was performed on QuantStudio™ 6 Flex system(ABI, Life, USA)
150 according to the manufacturer's instructions. The primers were synthesized by
151 Sangon Biotech(Shanghai, China). The relative expression levels of *PvGUX1_1* were
152 compared with that of β -actin, and the expression fold changes were calculated using
153 the $2^{-\Delta\Delta Ct}$ method. Each qRT-PCR reaction was performed in triplicate. Sequences of
154 the primers used for qRT-PCR in this study are shown in **Supplementary Table 2**.

155 **Variant calling and annotation**

156 The raw paired-end reads were initially filtered by fastp (v0.20.0) software with the
157 following parameters: -q 30. Next, the clean reads were aligned with the common
158 bean reference genome V2.1 (Schmutz et al., 2014) using MEM algorithm of BWA
159 (v0.7.17-r1188) (Li et al., 2009).

160 The tools SortSam and MarkDuplicates in PICARD (v1.127) were used to sort
161 mapping results and mark the duplicate reads (<https://broadinstitute.github.io/picard/>).
162 In addition, realignment around InDels was conducted by RealignerTargetCreator and
163 IndelRealigner in GATK (v3.2) (McKenna et al., 2010). The variant was called by the
164 UnifiedGenotyper module in GATK and SAMTOOLS (v1.6-3-g200708f) (Li et al.,
165 2009). The two variant results were combined and further filtered to obtain a credible
166 variant dataset using the GATK subcomponents SelectVariants and VariantFiltration.
167 The credible variant dataset was employed to recalibrate and realign results using the
168 BaseRecalibrator and PrintReads of GATK. The SNP and InDel were again called
169 against the recalibrated results. Finally, a vcf file including all samples and variants
170 was generated and further filtered using vcftools software (0.1.15) with the following
171 parameters: -max-missing 0.95 -maf 0.05 -min-alleles 2 -max-alleles 2 -recode
172 -recode-INFO-all.

173 The functional annotation of variants was performed using the software
174 ANNOVAR (Version:2017-07-17) (Wang et al., 2010).

175 **Population genetics analyses**

176 To analyze the population structure, the reduced SNPs were employed based on the
177 value of the correlation coefficient (r^2), where SNPs with strong linkage
178 disequilibrium (LD) ($r^2 > 0.2$) within a 50-kb window were discarded using plink
179 (v1.90b6) software with the following parameters: -indep-pairwise 50 10 0.2. To
180 estimate the most optimal sub-population, a cross-validation procedure was conducted
181 with ADMIXTURE (v1.3.0) runs from $K=2$ to 16 (Alexander et al., 2011). A
182 neighbor-joining tree of 138 snap bean accessions was constructed using Phylip 3.68
183 (Felsenstein et al., 1989) software based on a distance matrix. The bar plots of
184 sub-populations and the phylogenetic tree were plotted using the itol website
185 (<https://itol.embl.de/>).

186 **Linkage disequilibrium analysis**

187 The correlation coefficient (r^2) of pairwise SNPs within a 1000-kb window from all
188 chromosomes were used to estimate LD decay, which was calculated and plotted
189 using PopLDdecay software (Zhang et al., 2019). LDBlockShow software was used to

190 calculate and display LD blocks in candidate regions
191 (<https://github.com/BGI-shenzhen/LDBlockShow>).

192 **Genome-wide association analysis**

193 The high-quality SNPs were used for GWAS analysis in the R package GAPIT (Tang
194 et al., 2016). To reduce false positives and improve statistical power, the ‘Q+K’
195 approach was employed. The kinship matrix (K) was calculated with the default
196 method in GAPIT. The significant threshold ($-\log_{10}P$) was Bonferroni-corrected as
197 $-\log_{10}P=7.86$. The Manhattan plot was run by the CMplot package in R 3.6.1
198 (<https://github.com/YinLiLin/CMplot>).

199 **Analyses of collinearity and synteny**

200 The genome sequence information of common bean (*Phaseolus vulgaris* V2.1) and
201 cowpea (*Vigna angularis* V1.2) were downloaded from phytozome 13. The genomes
202 of soybean (*Glycine max* 109)
203 (www.plantgdb.org/XGDB/phplib/download.php?GDB=Gm) and pea (*Pisum*
204 *sativum*)
205 (<https://urgi.versailles.inra.fr/Species/Pisum>) were downloaded from public databases.
206 The analysis of collinearity and synteny between the four legumes was implemented
207 with MCScan (Python version)
208 ([https://github.com/tanghaibao/jcvi/wiki/MCscan-\[Python-version\]](https://github.com/tanghaibao/jcvi/wiki/MCscan-[Python-version])). The proteins
209 with similarity with over 90% on PvGUX1_1 in common bean, soybean, cowpea, and
210 pea were identified using BLASTP with an e value $<1e^{-5}$. The neighbor-joining tree
211 from the orthologue gene of *PvGUX1_1* was constructed using MEGA X (Kumar et
212 al., 2018) with default parameters.

213 **Results**

214 **Pod suture string phenotyping**

215 The pod suture strings of 138 snap bean accessions were investigated based on rating
216 and ratio (Figure 1). For rating, the presence of strings was defined as 1; the absence
217 of strings was defined as 0. The rating were investigated in 2019 (**Figure 1B**) and
218 2020 (**Figure 1D**). A total of 60 accessions were stringless, whereas 78 accessions
219 had suture strings in 2019 (ST2-2019) (**Figure 1B**). However, five accessions showed
220 different ratings in 2020 (ST2-2020). For ratio, the average ratio values (string
221 length/pod length) of 10 pods in each accession were measured in 2019 (ST1-19) and
222 2020 (ST1-20) (**Figures 1A,C**). The analysis of correlation for ratio showed that there
223 was a significantly high correlation of 0.93 ($P = 0.00015$) between 2019 and 2020.

224 **Resequencing of snap bean accessions**

225 The whole-genome resequencing of 138 accessions produced a total of 3.08 billion
226 raw paired-end reads and 0.92 Tb bases, which was approximately 11.4-fold sequence
227 depth, ranging from 10.2- to 13.5-fold. After being filtered, 2.71 billion clean reads
228 were retained. Mapping against the common bean genome V2.1 resulted in 5,130,030
229 SNPs and 1,524,528 InDels. Further filtering (bi-allelic, missing data < 0.05, minor
230 allele frequency >0.05) identified 3,656,683 high-confidence SNPs and 626,853
231 InDels. Among these variants, 3,589,978 SNPs and 618,666 InDels were placed on
232 chromosomes; 66,705 SNPs and 8187 InDels were on scaffolds. The distribution of
233 these SNPs across the genome was uneven (**Figure 2**). Most SNPs were located in
234 Chr02 (411,294), and the fewest SNPs were found in Chr06 (238,452). In addition,
235 the frequency of SNPs in Chr02 (8.28 SNPs/kb) was the highest, while the frequency
236 of SNPs in Chr08 (5.97 SNPs/kb) was the lowest (**Supplementary Table 3**).

237 To investigate distribution regions of these variants across the genome, we
238 carried out variant annotation and found that 146,882, 512,153, 279,102, and 244,805
239 SNPs and 4180, 53,742, 30,812, and 28,930 InDels were located in exons, introns,
240 upstream, and downstream, respectively. Furthermore, of these SNPs in exons, 65,001
241 nonsynonymous, 718 stopgain, and 171 stoploss InDels were annotated, which
242 resulted in amino acid changes, premature stop codons, or longer transcripts.
243 Similarly, of these InDels in exons, 697 frameshift insertion, 1091 frameshift deletion,
244 three stoploss, and 49 stopgain InDels were annotated, which also influenced protein
245 sequences.

246 **Population structure and LD analysis**

247 The analysis of population structure allows researchers to understand the genetic
248 relationships and origins of species. After removing the SNPs with strong LD ($r^2 \geq$
249 0.2), 97,841 SNPs were generated and used to implement population structure
250 analysis with Admixture. The use of $K = 2$ divided the 138 genotypes into two genetic
251 groups, which was in agreement with two domesticated genepools (Andean and
252 Middle American) (**Figure 3**). Among the 138 genotypes, 40 genotypes had
253 predominantly Andean ancestry, and 30 genotypes contained a level of hybridization,
254 suggesting that a high degree of intercrossing between the genepools that has
255 happened within snap beans.

256 We further analyzed the LD decay across the genome (**Supplementary Figure 1**).
257 The average LD decay of the whole genome was 631.4 kb (r^2 dropped to half of its
258 maximum value), which was faster than that of common bean (107 kb) (Wu et al.,
259 2020), cultivated soybean (150 kb) (Zhou et al., 2015), and cultivated rice (123 kb for
260 indica and 167 kb for japonica) (Huang et al., 2010). In addition, we found that the

261 rate of LD decay in different chromosomes varied from 184 kb (Chr10) to 976 kb
262 (Chr01) (**Supplementary Table 4**).

263 **Genome-wide association study for pod stringlessness**

264 To find out genetic loci controlling pod stringlessness, we implemented GWAS for
265 four traits (ST1-2019, ST2-2019, ST1-2020, and ST2-2020) using 3,656,683 SNPs
266 (**Figure 4**). The Q2 and relatedness kinship matrix as covariates were taken into
267 account to reduce false positives in GWAS analysis with a compressed mixed linear
268 model. The $-\log_{10}(P)=7.86$ was set as a genome-wide significance threshold based
269 on Bonferroni correction. Strong association signals were used to identify candidate
270 regions and screen candidate genes.

271 A total of 205 loci were identified with $-\log_{10}(P)>7.86$ for ST1-2019. Of 205
272 SNPs, 204 were located at Chr02, and one was located at Chr11 (**Supplementary**
273 **Table 5**). The peak signal was located at Chr02:44026689 ($-\log_{10}(P)=10.08$),
274 accounting for 14.53% of phenotypic variation. The major locus Chr02:44248269
275 ($-\log_{10}(P)=8.60$) was significantly associated with ST2-2019. Furthermore, strong
276 signals were both found at Chr02:44194640 for ST1-2020 ($-\log_{10}(P)=8.49$) and
277 ST2-2020 ($-\log_{10}(P)=9.62$). Taken together, the peak SNPs for four traits were all
278 located in adjacent physical regions in chromosome 2, which suggested the pod
279 stringlessness was under the control of a major locus.

280 **Identification of candidate genes for pod stringlessness**

281 To identify the candidate regions associated with the significant SNPs, we carried out
282 haplotype analysis in the whole genome. We found that these peak SNPs for the four
283 traits all resided on the same linkage disequilibrium (LD) block
284 (Chr02:43998258–44264446) (**Figure 5**). These genes located in the block were
285 likely responsible for the formation of stringlessness. **Table 1** shows these genes and
286 their homologous genes in Arabidopsis. A total of 23 putative genes were annotated in
287 this block based on the common bean reference genome V2.1. Eighteen out of 23
288 genes were functionally annotated, and 15 genes had homologous genes in
289 Arabidopsis. Furthermore, 102 SNPs, including 43 nonsynonymous and 59
290 synonymous SNPs, and 6 InDels, including two frameshift deletions distributed in the
291 coding areas of these genes, were also identified (**Table 2**).

292 A 2-bp deletion in the exon region was identified in *Phvul.002G270800*, an
293 ortholog to *AtGUX1*, which is responsible for secondary wall deposition in
294 Arabidopsis. The 2-bp deletion introduced a premature stop codon that truncated the
295 protein to 64 amino acids. To verify the deletion, we cloned the gene from two suture
296 and non-suture accessions (**Supplementary Figure 2**). The result was similar to the
297 finding in resequencing. Additionally, the deletion of 2 bp was significantly correlated

298 with pod stringlessness (2.2×10^{-16}) (**Figure 6**). We identified another a 2-bp deletion
299 in gene *Phvul.002G271600*; however, the function of this gene was unclear.

300 The most abundant nonsynonymous SNPs were found in *Phvul.002G271700*.
301 *Phvul.002G271700*, encoding a NAC domain protein, carried eight nonsynonymous
302 SNPs. Among these SNPs, K120I was significantly associated with pod stringlessness
303 (1.39×10^{-8}), whereas other SNPs exhibited weak association.

304 Three nonsynonymous SNPs, T32C, C604T and C737T, were identified in
305 *PvIND* (*Phvul.002G271000*). The SNPs T32C and C604 showed weak association (P
306 = 6.42×10^{-8} and 6.79×10^{-6}) with pod stringlessness, while C737T showed no
307 association ($P = 0.24$).

308 **Syntenic analysis of the candidate region between the common bean and other** 309 **legumes**

310 To identify the function and relation of the candidate gene, we performed
311 syntenic analysis within the candidate region of common bean with three legumes,
312 including soybean (*Glycine max*), cowpea (*Vigna angularis*), and pea (*Pisum sativum*).
313 Common bean, cowpea, and soybean are members of the Phaseoleae tribe, whereas
314 pea belongs to the Fabeae tribe (Dong et al., 2014). Amongst these legumes, the
315 majority of cowpea are stringless, while common bean and pea have stringless and
316 string types. In the Phaseoleae tribe, common bean and cowpea are the two most
317 closely related crop species of the four legumes analyzed. They also exhibited a high
318 degree of synteny (**Figure 7A**), in which 19 of 23 genes were orthologous. Although
319 large-scale synteny with soybean was also observed, the homologous genes in
320 soybean were divided into two regions (Glyma08g15530–Glyma08g15650 and
321 Glyma08g16570–Glyma08g16640) on chromosome 8. In contrast, the pea
322 chromosome exhibited a large rearrangement with common bean.

323 Overall, these candidate genes and gene order in common bean were highly
324 conserved and exhibited extensive synteny with cowpea. However, none of orthologs
325 for *Phvul.002G270800* in the syntenic block were identified (**Figure 7A**). To identify
326 the orthologous gene of *Phvul.002G270800* (*PvGUX1_1*), the protein of
327 *Phvul.002G270800* was used to conduct BLASTP search against cowpea, soybean,
328 pea, and common bean. Specifically, we identified another common bean protein,
329 *Phvul.009G148800* (*PvGUX1_2*), which shared a strong sequence homolog to
330 *PvGUX1_1*. *PvGUX1_2* encoded 636 amino acids, whereas *PvGUX1_1* encoded 221
331 amino acids. The best hit of *PvGUX1_1* in cowpea, *Vigun03g064600*, encoded 629
332 amino acids, which exhibited [large sequence difference with *PvGUX1_1*](#). To verify
333 the relationship between *PvGUX1_1*, *PvGUX1_2* and *GUX1*, we performed a
334 phylogenetic analysis of *PvGUX1_1*, *PvGUX1_2*, and other orthologous genes.

335 PvGUX1_1 and PvGUX1_2 were placed in two different sub-branches (**Figure 7B**).
336 Although the corresponding genes, Glyma08g15640 and Vigun03g064600, in the
337 synteny region were clustered with PvGUX1_1 in one sub-branch, there was large
338 sequence variation between PvGUX1_1 and other orthologs. Collectively, these data
339 demonstrated that PvGUX1_1 and PvGUX1_2 diverged at an early stage in legume
340 evolution, which may have resulted in gene diversification.

341 **Gene expression patterns of PvGUX1_1**

342 The formation of pod sutures is an important agronomic trait. To better reveal the
343 genetic regulation of pod sutures, we conducted qRT-PCR analysis of PvGUX1_1 at
344 the initiation of pod elongation (T1, no suture), pod development (T2, no suture), and
345 pod maturation (T3, sutures were present in sutured pods) for sutured (R05) and
346 non-sutured pods (R02) (**Figure 7D**). The qRT-PCR results indicated that the
347 expression levels of PvGUX1_1 were significantly higher at the T1 and T2 stages in
348 non-sutured pods compared with the sutured pods (**Figure 7E**). Furthermore, the
349 expression level of PvGUX1_1 decreased following the development of pods in
350 non-sutured pods (**Figure 7C**).

351 **Discussion**

352 Understanding the genetic mechanism of suture string development will facilitate the
353 study of domestication and plant breeding in snap bean. Here, we identified a strong
354 signal on Chr02 that determined the formation of pod stringlessness based on
355 large-scale resequencing. Within these putative genes in candidate regions,
356 *PvGUX1_1* was the best candidate gene due to its function and polymorphisms, which
357 was consistent with dominant inheritance.

358 **GWAS analysis for pod stringlessness**

359 As common bean is a selfing species, effective recombination and heterozygosity in
360 common bean are significantly reduced, which results in the generation of large LD
361 and slow LD decay. Generally, LD decay is slower in selfing species than in
362 outcrossing species because of the loss of recombination, which potentially leads to
363 be homozygosity (Morrell et al., 2012). The nature of homozygosity makes common
364 bean access to design GWAS. In particular, once a genotype is sequenced, the
365 phenotype can be investigated in different environments. Moreover, the extensive
366 genetic diversity is advantageous for GWAS analysis in common bean (Blair et al.,
367 2009).

368 **Pod stringlessness was controlled by a major locus**

369 The inheritance of pod stringlessness is complex due to genotype and environmental
370 factors (Ma et al., 2016). Since the stringless trait was observed, various inheritance
371 models for stringless trait in common bean have been proposed. Currence (1930)
372 assumed that two genes (S for dominant, T epistatic to S) regulated the stringless trait.
373 However, more studies revealed that the stringless trait was under the control of a
374 single dominant locus (*St*), which was mapped on chromosome 2 (Koinange et al.,
375 1996; Davis et al., 2006; Gioia et al., 2012). Moreover, there have also been reports
376 that the trait did not fit the ratio of one or more loci, and thus was a quantitative trait
377 (Hagerty et al., 2016). In order to verify the inheritance pattern, qualitative traits and
378 quantitative traits were both used for GWAS analysis. Interestingly, we obtained
379 similar results from the two models. The only strong signal from both models was
380 identified on Chr02, which was in agreement with previous findings, and showed that
381 the formation of suture string was controlled by a major locus.

382 The formation of suture string is controlled by a single locus, while the level
383 (short versus long) of the string might be more complex. This characteristic was also
384 observed in pod shattering. As suggested by Rau et al., (2019), at least two additional
385 loci were likely relevant to the level and mode of pod shattering. In our study, in
386 addition to Chr02, a SNP located at Chr11 was also associated with stringlessness
387 (**Supplementary Figure 3**). The SNP was about 0.13 Mb from the NAC transcription
388 factor gene *PvCUC2* (*Phvul.011G160400*, Chr11:45614432_45616861). In order to
389 identify more locus, we conducted GWAS only on stringy snap bean for ST1-2019.
390 Strong association signals were identified on Chromosome 7 (Supplementary Figure
391 4). These locus may be responsible for the level of suture string, along with the *St*
392 gene. This finding supported the hypothesis by Drijfhout (1978) that a major factor
393 influenced the string formation trait, while other genes led to incomplete strings.

394 **Candidate gene for stringlessness in snap bean**

395 A total of 23 genes within the LD block surrounding the high association signal were
396 identified. Among them, several genes are orthologous genes involved in cell-wall
397 biosynthesis, pod shattering, and fiber formation. *Phvul.002G270800* is the
398 orthologous gene of *AtGUX1* (*AT3G18660*). In Arabidopsis, *AtGUX1* belongs to
399 Glycosyltransferase Family 8, which participates in the synthesis of plant cell walls
400 (Yin et al., 2010). *AtGUX1* is responsible for the decoration of xylan, an important
401 component of the secondary cell wall (Lee et al., 2012). Silencing *AtGUX1* led to the
402 decrease of glucuronoxylan content and microsomal xylan in the cell wall (Oikawa et
403 al., 2010). In our study, a 2-bp deletion was found in the exon region of
404 *Phvul.002G270800*, causing a premature stop. The 2-bp deletion was significantly

405 associated with pod stringlessness. Therefore, we propose *Phvul.002G270800* as the
406 best candidate gene for *St* locus.

407 In addition to *Phvul.002G270800*, another gene of interest was
408 *Phvul.002G271000*, the orthologous gene to *AtIND*. *AtIND*, as a b-HLH transcription
409 factor, plays a crucial role in pod shattering in *Arabidopsis* (Girin et al., 2010; Kay et
410 al., 2013; Dong and Wang, 2015). However, due to the lack of mutation in *PvIND*
411 (*Phvul.002G270800*), a previous study reported that it was not the *St* gene controlling
412 suture strings (Gioia et al., 2012). Although the present study identified three
413 nonsynonymous SNPs in the exon region of *PvIND*, these SNPs only showed a weak
414 association with the suture strings. Therefore, *PvIND* may not be directly involved in
415 suture development. Other interesting genes included NAC transcription factor
416 *Phvul.002G271700* (*PvVNII*) and MYB transcription factor *Phvul.002G269900*
417 (*PvMAMYB*). Many studies have suggested that an NAC transcription factor is
418 correlated with pod shattering and secondary cell wall development (Hussey et al.,
419 2011; Yamaguchi et al., 2010; Reusche et al., 2012). In particular, the role of the
420 NAC transcription factor SHA1-5 in regulating pod shattering in soybean has been
421 elucidated in detail (Dong et al., 2014). Likewise, several MYB transcription factors,
422 such as *MYB26* (Wilson et al., 2011), *MYB46* (Kim et al., 2013,2014), and *MYB63*
423 (Zhou et al., 2009), are involved in lignin biosynthesis and secondary cell wall
424 formation in many species (Nakano et al., 2015). Therefore, the functions of *PvVNII*
425 and *PvMAMYB* need to be further studied in future research to determine whether
426 they are related to suture string development or pod shattering.

427 **Pod stringlessness in other legumes**

428 The loss or presence of suture strings is not an important factor for many legumes in
429 which the dry seeds are consumed. In legumes, reports on the stringless trait are
430 currently only found in common bean and pea. In pea, pod stringlessness arose from
431 spontaneous mutation (Wellensiek, 1971). The recessive gene (*sin-2*) is regarded as
432 the key gene responsible for the stringless trait in pea (McGee and Baggett, 1992; Ma
433 et al., 2016). In contrast, the stringless trait in common bean is governed by the
434 dominant gene *St*. In the synteny block, the orthologs of *GUXI* were not detected in
435 pea, indicating that the genetic mechanism of stringlessness between the two legumes
436 may be different.

437 Although the same regulation gene may not be shared in common bean and pea,
438 there are many parallels, including seed dormancy, growth habit, and earliness,
439 between common bean and pea that have occurred in the process of crop
440 domestication (Weeden, 2007). The identification of the *St* gene in common bean

441 would accelerate the mining of *sin-2* and improve the understanding of the genetics of
442 domestication under parallel selection in the future.

443 **Data Availability Statement**

444 The original contributions presented in the study are included in the
445 article/Supplementary Material, further inquiries can be directed to the corresponding
446 author.

447 **Author Contributions**

448 QW designed the study. LZ and GS conducted the experiments. LZ, ZH, and XZ
449 analyzed the data. LZ wrote the manuscript. QW, XZ, ZH, and GS revised the
450 manuscript.

451 **Funding**

452 This work was performed at the Key Laboratory of Agriculture, Beijing, China, and
453 was supported by the Chinese Academy of Agricultural Sciences Innovation Project
454 (CAAS-ASTIP-IVFCAAS), Key Laboratory of Biology and Genetic Improvement of
455 Horticultural Crops, Ministry of Agriculture, Beijing, China.

456 **Conflict of interest**

457 The authors declare that the research was conducted in the absence of any commercial
458 or financial relationships that could be construed as a potential conflict of interest.

459 **Supplementary Material**

460 The Supplementary Material for this article can be found online.

461 **References**

- 462 Alexander, D. H., and Lange, K. (2011) Enhancements to the admixture algorithm for
463 individual ancestry estimation. *BMC Bioinformatics*. 12(1): 1-6.
464 doi:10.1186/1471-2105-12-246
- 465 Blair, M. W., Astudillo, C., Grusak, M. A., Graham, R., and Beebe, S. E. (2009)
466 Inheritance of seed iron and zinc concentrations in common bean (*Phaseolus*
467 *vulgaris* L.). *Molecular Breeding* 23(2):197-207.
468 doi:10.1007/s11032-008-9225-z.
- 469 Currence, T. M. (1930) Inheritance studies in *Phaseolus vulgaris*. *Tech Bull Minn*
470 *Agric Exp Stn* 68:1-28
- 471 Davis, J. W., Kean, D., Yorgey, B., Fourie, D., Miklas, P. N., and Myers, J. R. (2006)
472 A molecular marker linkage map of snap bean (*Phaseolus vulgaris*). *ANNUAL*
473 *REPORT-BEAN IMPROVEMENT COOPERATIVE* 49:73

- 474 Delfini, J., Moda-Cirino, V., dos Santos Neto, J., Zeffa, D. M., Nogueira, A. F., and
475 Ribeiro, L. A. B., et al. (2021) Genome-wide association study for grain mineral
476 content in a Brazilian common bean diversity panel. *Theor Appl Genet*
477 134:2795-2811. doi:10.1007/s00122-021-03859-2
- 478 Di Vittori, V., Bitocchi, E., Rodriguez, M., Alseekh, S., Bellucci, E., and Nanni, L., et
479 al. (2020) Pod indehiscence in common bean is associated to the fine regulation
480 of PvMYB26 and a non-functional abscission layer. *Journal of experimental*
481 *botany* 72(5):1617-1633. doi:10.1093/jxb/eraa553
- 482 Dong, Y., and Wang, Y. Z. (2015) Seed shattering: from models to crops. *Frontiers in*
483 *Plant Science* 6: 476. doi: 10.3389/fpls.2015.00476
- 484 Dong, Y., Yang, X., Liu, J., Wang, B-H., Liu, B-L., and Wang, Y-Z. (2014) Pod
485 shattering resistance associated with domestication is mediated by a NAC gene
486 in soybean. *Nat. Commun* 5:3352. doi:10.1038/ncomms4352
- 487 Drijfhout, E. (1978) Inheritance of temperature-dependent string formation in
488 common bean (*Phaseolus vulgaris* L.). *Netherlands Journal of Agricultural*
489 *Science* 26(1):99-105. doi:10.18174/njas.v26i1.17114
- 490 Felsenstein, J. (1989) PHYLIP—Phylogeny Inference Package (Version 3.2).
491 *Cladistics* 5:164–166. <https://www.jstor.org/stable/2830216>
- 492 Gioia, T., Logozzo, G., Kami, J., Zeuli, P. S., and Gepts, P. (2012) Identification and
493 characterization of a homologue to the Arabidopsis INDEHISCENT gene in
494 common bean. *Journal of Heredity* 104(2):273-286. doi:10.1093/jhered/ess102
- 495 Girin, T., Stephenson, P., Goldsack, C. M., Kempin, S. A., Perez, A., and Pires, N., et
496 al. (2010) Brassicaceae INDEHISCENT genes specify valve margin cell fate and
497 repress replum formation. *The Plant Journal* 63(2):329-338.
498 doi:10.1111/j.1365-313X.2010.04244.x
- 499 Hagerty, C. H., Cuesta-Marcos, A., Cregan, P., Song, Q., McClean, P., and Myers, J. R.
500 (2016) Mapping snap bean pod and color traits, in a dry bean × snap bean
501 recombinant inbred population. *Journal of the American Society for*
502 *Horticultural Science* 141(2):131-138. doi:10.21273/JASHS.141.2.131
- 503 Huang, X., Sang, T., Zhao, Q., Feng, Q., Zhao, Y., and Li, C., et al. (2010)
504 Genome-wide association studies of 14 agronomic traits in rice landraces. *Nature*
505 *genetics* 42(11):961-967. doi:10.1038/ng.695
- 506 Hussey, S. G., Mizrachi, E., Spokevicius, A. V., Bossinger, G., Berger, D. K., and
507 Myburg, A. A. (2011) SND2, a NAC transcription factor gene, regulates genes
508 involved in secondary cell wall development in Arabidopsis fibres and increases
509 fibre cell area in Eucalyptus. *BMC plant biology* 11(1): 173.
510 doi:10.1186/1471-2229-11-173
- 511 Kamfwa, K., Cichy, K. A., and Kelly, J. D. (2015) Genome-wide association study of
512 agronomic traits in common bean. *The Plant Genome* 8(2):1-12.
513 doi:10.3835/plantgenome2014.09.0059
- 514 Kay, P., Groszmann, M., Ross, J. J., Parish, R. W., and Swain, S. M. (2013)
515 Modifications of a conserved regulatory network involving INDEHISCENT
516 controls multiple aspects of reproductive tissue development in Arabidopsis. *New*
517 *Phytologist* 197(1):73-87. doi:10.1111/j.1469-8137.2012.04373.x

- 518 Kim, W. C., Kim, J. Y., Ko, J. H., Kang, H., and Han, K. H.(2014) Identification of
519 direct targets of transcription factor MYB46 provides insights into the
520 transcriptional regulation of secondary wall biosynthesis. *Plant molecular*
521 *biology* 85(6):589-599. doi:10.1007/s11103-014-0205-x
- 522 Kim, W. C., Ko, J. H., Kim, J. Y., Kim, J., Bae, H. J., and Han, K. H. (2013) MYB 46
523 directly regulates the gene expression of secondary wall-associated cellulose
524 synthases in *A. rabidopsis*. *The Plant Journal* 73(1):26-36.
525 doi:10.1111/j.1365-313x.2012.05124.x
- 526 Koinange, E. M., Singh, S. P., and Gepts, P. (1996) Genetic control of the
527 domestication syndrome in common bean. *Crop Science* 36(4):1037-1045.
528 doi:10.2135/cropsci1996.0011183X003600040037x
- 529 Kumar, S., Stecher, G., Li, M., Knyaz, C., and Tamura, K. (2018) MEGA X:
530 molecular evolutionary genetics analysis across computing platforms. *Molecular*
531 *biology and evolution*, 35(6):1547-1549. doi:10.1093/molbev/msy096
- 532 Lee, C., Teng, Q., Zhong, R., and Ye, Z. H. (2012) Arabidopsis GUX proteins are
533 glucuronyltransferases responsible for the addition of glucuronic acid side chains
534 onto xylan. *Plant and Cell Physiology* 53(7):1204-1216. doi:10.1093/pcp/pcs064
- 535 Li, H., and Durbin, R. (2009) Fast and accurate short read alignment with
536 Burrows-Wheeler transform. *bioinformatics* 25(14):1754-1760.
537 doi:10.1093/bioinformatics/btp324
- 538 Ma, Y., Hu, J., Myers, J. R., Mazourek, M., Coyne, C. J., and Main, D., et al. (2016)
539 Development of SCAR markers linked to sin-2, the stringless pod trait in pea
540 (*Pisum sativum* L.). *Molecular Breeding* 36(7):1-10.
541 doi:10.1007/s11032-016-0525-4
- 542 McGee, R. J., and Baggett, J. R. (1992) Inheritance of Stringless Pod in *Pisum*
543 *sativum* L. *Journal of the American Society for Horticultural*
544 *Science*, 117(4):628-632. doi:10.21273/JASHS.117.4.628
- 545 McKenna, A., Hann,a M., Banks, E., Sivachenko, A., Cibulskis, K., and Kernytsky, A.,
546 et al. (2010) The Genome Analysis Toolkit: a MapReduce framework for
547 analyzing next-generation DNA sequencing data. *Genome*
548 *research* 20(9):1297-1303. doi:10.1101/gr.107524.110
- 549 Moghaddam, S. M., Mamidi, S., Osorno, J. M., Lee, R., Brick, M., and Kelly, J., et al.
550 (2016) Genome-wide association study identifies candidate loci underlying
551 agronomic traits in a Middle American diversity panel of common bean. *The*
552 *Plant Genome* 9(3):1-21. doi:10.3835/plantgenome2016.02.0012.
- 553 Morrell, P. L., Buckler, E. S., and Ross-Ibarra, J. (2012) Crop genomics: advances and
554 applications. *Nature Reviews Genetics* 13(2):85-96. doi:10.1038/nrg3097
- 555 Myers, J. R., and Kmiecik, K. (2017) Economic importance and relevance to
556 biological science research. In: *The common bean genome*. Springer, Berlin, pp
557 1-20. doi:10.1007/978-3-319-63526-2_1
- 558 Myers, J. R., Wallace, L. T., Moghaddam, S. M., Kleintop, A. E., Echeverria, D., and
559 Thompson, H. J, et al. (2019) Improving the Health Benefits of Snap Bean:
560 Genome-Wide Association Studies of Total Phenolic
561 Content. *Nutrients* 11(10):2509. doi:10.3390/nu11102509

- 562 Nakano, Y., Yamaguchi, M., Endo, H., Rejab, N. A., and Ohtani, M. (2015)
563 NAC-MYB-based transcriptional regulation of secondary cell wall biosynthesis
564 in land plants. *Frontiers in plant science*, 6:288. doi:10.3389/fpls.2015.00288
- 565 Oikawa, A., Joshi, H. J., Rennie, E. A., Ebert, B., Manisseri, C., and Heazlewood, J.
566 L., et al. (2010) An integrative approach to the identification of Arabidopsis and
567 rice genes involved in xylan and secondary wall development. *PLoS One*
568 5(11):e15481. doi:10.1371/journal.pone.0015481
- 569 Parker, T. A., Berny, Mier y Teran, J. C., Palkovic, A., Jernstedt, J., and Gepts, P.
570 (2020) Pod indehiscence is a domestication and aridity resilience trait in
571 common bean. *New Phytol* 225:558–570. doi:10.1111/nph.16164
- 572 Prakken, R. (1934) Inheritance of colours and pod characters in *Phaseolus vulgaris*
573 L. *Genetica* 16(3-4):177-296.
- 574 Raggi, L., Caproni, L., Carboni, A., and Negri, V. (2019) Genome-wide association
575 study reveals candidate genes for flowering time variation in common bean
576 (*Phaseolus vulgaris* L.). *Frontiers in plant science* 10:962.
577 doi:10.3389/fpls.2019.00962
- 578 Rau, D., Murgia, M. L., Rodriguez, M., Bitocchi, E., Bellucci, E., Fois, D., et al.
579 (2019) Genomic dissection of pod shattering in common bean: mutations at
580 non-orthologous loci at the basis of convergent phenotypic evolution under
581 domestication of leguminous species. *The Plant Journal* 97(4):693-714.
582 doi:10.1111/tpj.14155
- 583 Reusche, M., Thole, K., Janz, D., Truskina, J., Rindfleisch, S., and Drübert, C., et al.
584 (2012) Verticillium infection triggers VASCULAR-RELATED NAC
585 DOMAIN7-dependent de novo xylem formation and enhances drought tolerance
586 in Arabidopsis. *The Plant Cell* 24(9):3823-3837. doi: 10.1105/tpc.112.103374.
587 doi:10.1105/tpc.112.103374
- 588 Schmutz, J., McClean, P. E., Mamidi, S., Wu, G. A., Cannon, S. B., and Grimwood, J.,
589 et al. (2014) A reference genome for common bean and genome-wide analysis of
590 dual domestications. *Nature genetics* 46(7):707-713. doi:10.1038/ng.3008
- 591 Soltani, A., MafiMoghaddam, S., Oladzad-Abbasabadi, A., Walter, K., Kearns, P. J.,
592 and Vasquez-Guzman, J., et al. (2018) Genetic analysis of flooding tolerance in
593 an Andean diversity panel of dry bean (*Phaseolus vulgaris* L.). *Frontiers in plant*
594 *science* 9:767. doi:10.3389/fpls.2018.00767
- 595 Tang, Y., Liu, X., Wang, J., Li, M., Wang, Q., and Tian, F., et al. (2016) GAPIT
596 version 2: an enhanced integrated tool for genomic association and
597 prediction. *The plant genome* 9(2):1-9. doi:10.3835/plantgenome2015.11.0120
- 598 Wang, K., Li, M., and Hakonarson, H. (2010) ANNOVAR: functional annotation of
599 genetic variants from high-throughput sequencing data. *Nucleic acids research*
600 38(16):e164-e164. doi:10.1093/nar/gkq603
- 601 Weeden, N. F. (2007) Genetic changes accompanying the domestication of *Pisum*
602 *sativum*: is there a common genetic basis to the ‘domestication syndrome’ for
603 legumes?. *Annals of botany* 100(5):1017-1025. doi:10.1093/aob/mcm122
- 604 Wellensiek, S. J. (1971) Lamprecht's gene sin for stringless. *Pisum Newsletter* 3:48.

- 605 Wilson, Z. A., Song, J., Taylor, B., and Yang, C. (2011) The final split: the regulation
606 of anther dehiscence. *Journal of experimental botany* 62(5):1633-1649.
607 doi:10.1093/jxb/err014
- 608 Wu, L., Chang, Y., Wang, L., Wang, S., and Wu, J. (2021) The aquaporin gene
609 PvXIP1;2 conferring drought resistance identified by GWAS at seedling stage in
610 common bean. *Theor Appl Genet* 1:16. doi:10.1007/s00122-021-03978-w
- 611 Wu, J., Wang, L., Fu, J., Chen, J., Wei, S., and Zhang, S., et al. (2020) Resequencing
612 of 683 common bean genotypes identifies yield component trait associations
613 across a north-south cline. *Nature Genetics* 52(1):118-125.
614 doi:10.1038/s41588-019-0546-0
- 615 Wu, J., Zhu, J., Wang, L., and Wang, S. (2017) Genome-wide association study
616 identifies NBS-LRR-encoding genes related with anthracnose and common
617 bacterial blight in the common bean. *Frontiers in plant science* 8:1398.
618 doi:10.3389/fpls.2017.01398
- 619 Yamaguchi, M., Goué, N., Igarashi, H., Ohtani, M., Nakano, Y., and Mortimer, J. C.,
620 (2010) VASCULAR-RELATED NAC-DOMAIN6 and VASCULAR-RELATED
621 NAC-DOMAIN7 effectively induce transdifferentiation into xylem vessel
622 elements under control of an induction system. *Plant physiology* 153(3):906-914.
623 doi:10.1104/pp.110.154013
- 624 Yin, Y., Chen, H., Hahn, M. G., Mohnen, D., and Xu, Y. (2010) Evolution and
625 function of the plant cell wall synthesis-related glycosyltransferase family
626 8. *Plant Physiology* 153(4):1729-1746. doi:10.1104/pp.110.154229
- 627 Zhang, X., Blair, M.W., and Wang, S. (2008) Genetic diversity of Chinese common
628 bean (*Phaseolus vulgaris* L.) landraces assessed with simple sequence repeat
629 markers. *Theor Appl Genet* 117: 629–640. doi:10.1007/s00122-008-0807-2
- 630 Zhang, C., Dong, S., Xu, J., He, W., and Yang, T. (2019) PopLDdecay: a fast and
631 effective tool for linkage disequilibrium decay analysis based on variant call
632 format files. *Bioinformatics*, 35(10):1786-1788.
633 doi:10.1093/bioinformatics/bty875
- 634 Zhou, Z., Jiang, Y., Wang, Z., Gou, Z., Lyu, J., and Li, W. (2015) Resequencing 302
635 wild and cultivated accessions identifies genes related to domestication and
636 improvement in soybean. *Nature biotechnology* 33(4):408-414.
637 doi:10.1038/nbt.3096
- 638 Zhou, J., Lee, C., Zhong, R., and Ye, Z-H. (2009) MYB58 and MYB63 are
639 transcriptional activators of the lignin biosynthetic pathway during secondary
640 cell wall formation in Arabidopsis. *The Plant Cell*
641 21(1):248-266. doi:10.1105/tpc.108.063321
- 642
- 643
- 644
- 645
- 646
- 647
- 648

649 **Figure legends**

650 **Figure. 1 Histograms of pod suture strings in 138 snap bean accessions.** (A) The
651 ratio (string length/pod length) was measured in 2019. (B) The rating (1 for the
652 presence of a string, and 0 for the absence of a string) was counted in 2019. (C) The
653 ratio was measured in 2020. (D) The rating was counted in 2020.

654 **Figure. 2 The number of SNPs within a 1-Mb window size across common bean**
655 **chromosomes.**

656 **Figure. 3 Neighbor-joining tree and population structure analysis using 97,841**
657 **single-nucleotide polymorphisms (SNPs).** The genepools are colored with red for
658 Andean and blue for Mesoamerican ancestry.

659 **Figure. 4 Circular Manhattan plots of a genome-wide association study (GWAS)**
660 **for pod stringlessness.** The inner circle to the outer circle represent ST1-2019,
661 ST2-2019, ST1-2020, and ST2-2020, respectively. The red dashed lines of each circle
662 indicate the threshold (7.86). Single-nucleotide polymorphisms (SNPs) over the
663 threshold are highlighted.

664 **Figure. 5 Manhattan plots and linkage disequilibrium (LD) heatmap over 266.29**
665 **kb around significant single-nucleotide polymorphisms (SNPs) on chromosome 2.**
666 (A) Manhattan plots of ST1-2019. The red dashed line represents the threshold (7.86).
667 SNPs over the threshold are highlighted in red. (B) Annotated genes in the region.
668 These CDS, introns, UTR, and intergenic regions are shown in green, light blue, pink,
669 and orange, respectively. (C) The LD heatmap over the region. Colors are coded
670 according to the r^2 color key.

671 **Figure. 6 The identification of a 2-bp deletion in Phvul.002G270800.** (a) Structure
672 of Phvul.002G270800. The red base represents the 2-bp deletion in
673 Phvul.002G270800. (b) Box plot of the ratio of string length/pod length for the 2-bp
674 deletion in Phvul.002G270800.

675 **Figure. 7 The analysis of phylogeny and expression of PvGUX1.** A. Syntenic
676 analysis of the candidate region between common bean and other legumes. B.
677 Phylogenetic tree for PvGUX1. Colors located at the right side of each sequence
678 represent their amino-acid composition. C. Gene expression of *PvGUX1_1* at different
679 pod development stages for string and stringless snap bean. D. Morphology of
680 stringless and string pod development stages T1–T3. E. The gene expression of
681 *PvGUX1_1* at three pod development stages. *P* values were calculated using student's
682 t test (* $p < 0.05$, ** $p < 0.01$).

683

684

685

686

687 Table 1. Putative genes in the 266.19 kb of candidate region

688

Gene	Positon	Homologs of Arabidopsis	Functional annotation
Phvul.002G269700	Chr02:44022772_44024106		Unknown
Phvul.002G269800	Chr02:44033313_44034850	AT4G08250	GRAS family transcription factor
Phvul.002G269900	Chr02:44036772_44037686	AT5G45420	MYB transcription factor
Phvul.002G270000	Chr02:44037878_44041667	AT3G18750	WNK family of protein kinases
Phvul.002G270100	Chr02:44042454_44059878	AT3G18730	Involved in cell division control and plant morphogenesis
Phvul.002G270200	Chr02:44066265_44067018	AT5G64667	Involved in floral organ abscission
Phvul.002G270300	Chr02:44080456_44082336	AT5G64660	CYS, MET, PRO, and GLY protein
Phvul.002G270400	Chr02:44125511_44131328	AT5G24320	Transducin/WD40 repeat-like superfamily protein
Phvul.002G270500	Chr02:44133980_44137288	AT3G18680	UMP Kinase
Phvul.002G270600	Chr02:44139105_44139713	AT3G18690	Involved in mediating responses to pathogens
Phvul.002G270700	Chr02:44142989_44144630	AT4G14620	Unknown
Phvul.002G270800	Chr02:44150261_44150926	AT3G18660	Encodes a glucuronyltransferase responsible for the addition of GlcA residues onto xylan and for secondary wall deposition.
Phvul.002G270900	Chr02:44155318_44157803	AT5G09760	Plant invertase/pectin methylesterase inhibitor
Phvul.002G271000	Chr02:44186987_44188326	AT4G00120	IND(basic helix-loop-helix (bHLH) DNA-binding superfamily protein)
Phvul.002G271100	Chr02:44199222_44205529	AT1G48880	Encodes a member of the TBL
Phvul.002G271200	Chr02:44205946_44210215	AT5G64630	Involved in organization of the shoot and root apical meristems.
Phvul.002G271300	Chr02:44216969_44222195		Unknown
Phvul.002G271400	Chr02:44224184_44228271	AT1G08490	Chloroplastic NifS-like protein
Phvul.002G271500	Chr02:44229799_44246330	AT5G64070	Encodes a phosphatidylinositol 4-OH kinase
Phvul.002G271600	Chr02:44232557_44233756		Unknown
Phvul.002G271700	Chr02:44247536_44251023	AT5G09330	NAC domain containing protein
Phvul.002G271800	Chr02:44251436_44254178	AT2G13690	PRLI-interacting factor
Phvul.002G271900	Chr02:44257054_44258132		Unknown

689

690

691

692

693

694

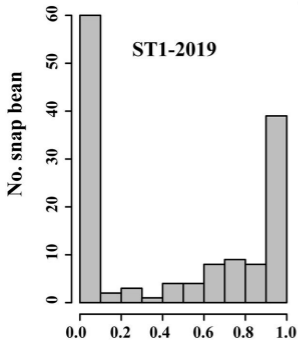
695

696 Table 2 Functional annotation information of candidate genes

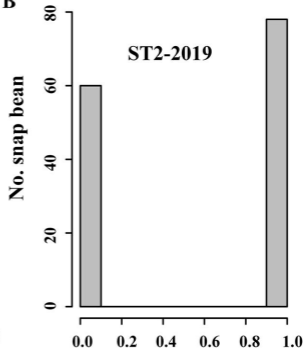
Gene	Variant Type	Base Change	Amino Change
Phvul.002G269700	Nonsynonymous	A491G	E164G
	Nonsynonymous	T1617A	D539E
Phvul.002G270100	Nonsynonymous	A1899T	R633S
	Nonsynonymous	G2092A	D698N
Phvul.002G270300	Nonsynonymous	C3050T	S1017L
	Nonsynonymous	C257T	S86L
Phvul.002G270400	Nonsynonymous	T382C	F128L
	Nonsynonymous	G563A	R188K
Phvul.002G270800	Nonsynonymous	C833A	T278N
	Nonsynonymous	A92G	D31G
Phvul.002G270900	Frameshift deletion	AT163_	
	Nonsynonymous	G1374C	E458D
Phvul.002G271000	Nonsynonymous	T32C	V11A
	Nonsynonymous	C604T	P202S
Phvul.002G271100	Nonsynonymous	C737T	T246M
	Nonsynonymous	A257G	N86S
Phvul.002G271200	Nonsynonymous	G870A	M290I
	Nonsynonymous	G241T	G81C
Phvul.002G271300	Nonsynonymous	A638C	E213A
	Nonsynonymous	A781G	T261A
Phvul.002G271400	Nonsynonymous	T1945G	S649A
	Nonsynonymous	A2008G	N670D
Phvul.002G271600	Nonsynonymous	G234A	M78I
	Nonsynonymous	A335C	K112T
Phvul.002G271700	Nonsynonymous	C902T	A301V
	Nonsynonymous	A1099G	T367A
Phvul.002G271800	Nonsynonymous	T17C	L6S
	Nonsynonymous	A24C	L8F
Phvul.002G271900	Frameshift deletion	GT57_	
	Nonsynonymous	A77G	N26S
Phvul.002G271900	Nonsynonymous	C78G	N26K
	Nonsynonymous	T100G	F34V
Phvul.002G271900	Nonsynonymous	T154C	S52P
	Nonsynonymous	G162C	K54N
Phvul.002G271900	Nonsynonymous	A359T	K120I
	Nonsynonymous	T476C	V159A
Phvul.002G271900	Nonsynonymous	A785C	D262A
	Nonsynonymous	A1346C	Y449S
Phvul.002G271900	Nonsynonymous	A1138C	K380Q
	Nonsynonymous	A772C	N258H
Phvul.002G271900	Nonsynonymous	T563A	F188Y
	Nonsynonymous	A385G	N129D
Phvul.002G271900	Nonsynonymous	C328A	L110M
	Nonsynonymous	T5G	F2C
Phvul.002G271900	Nonsynonymous	T377C	V126A

697

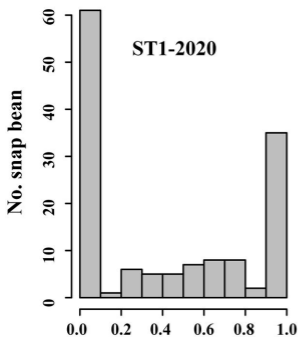
A



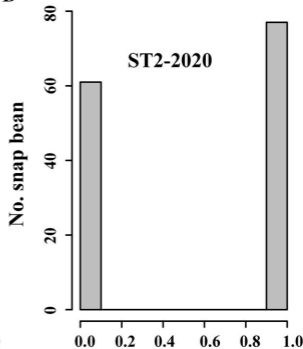
B



C

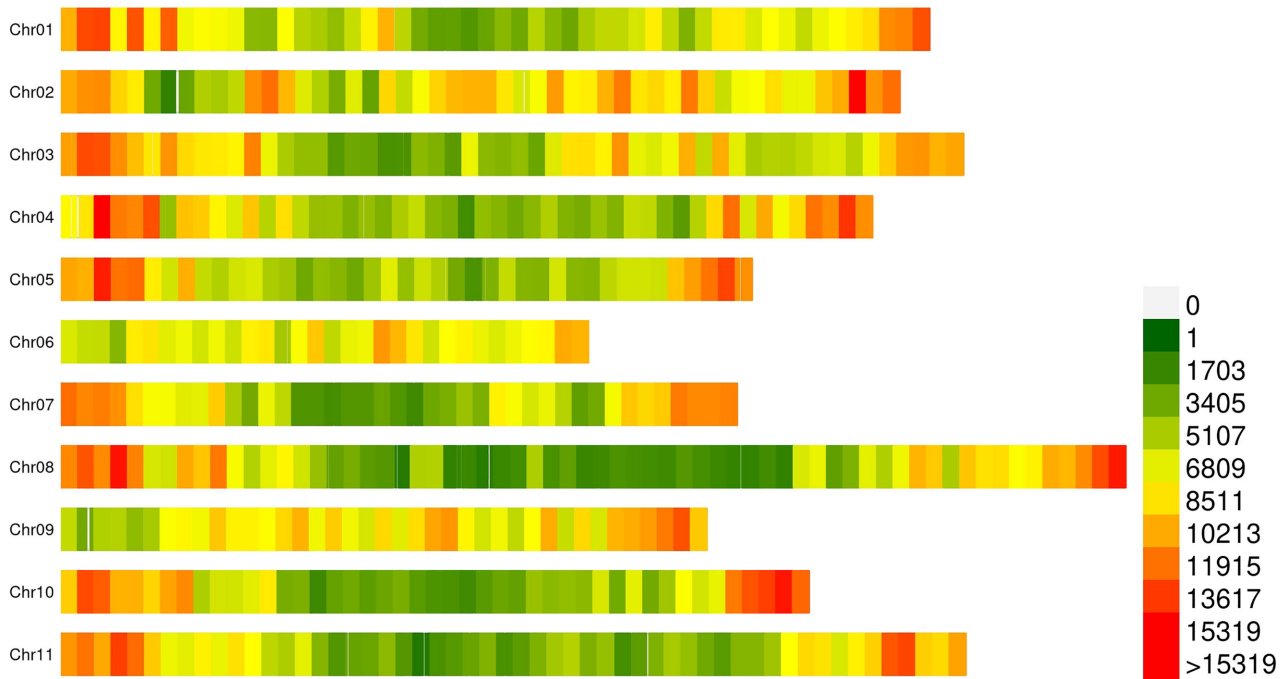


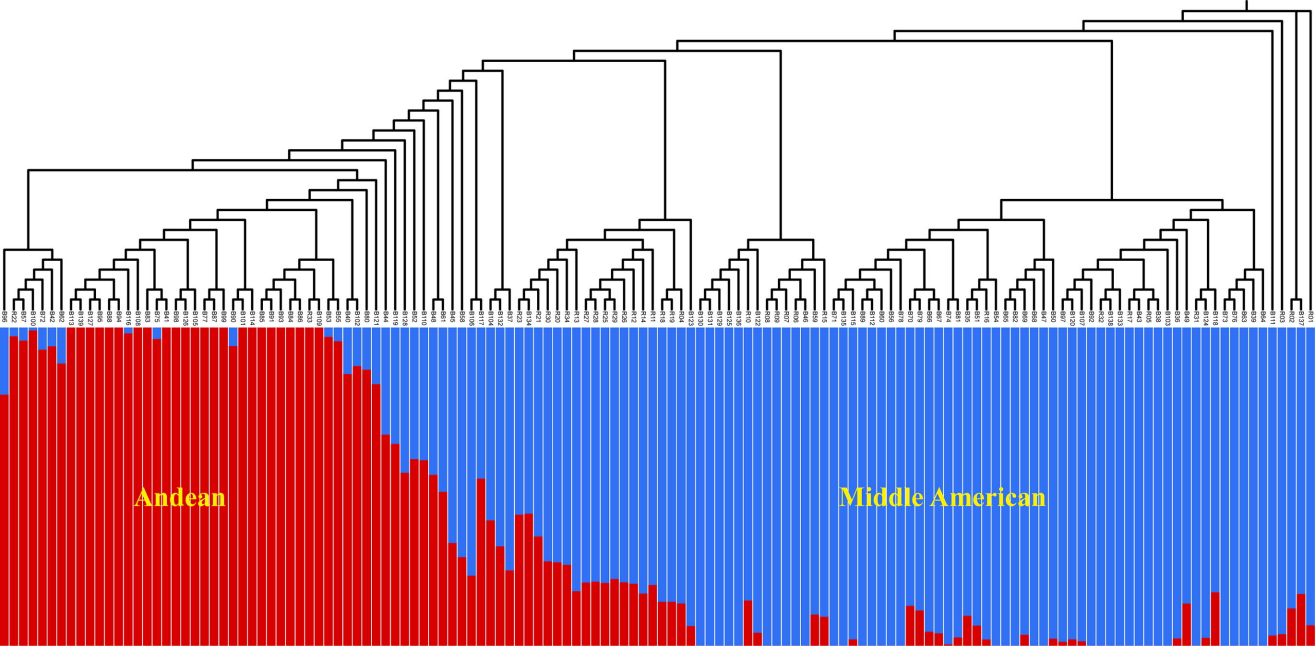
D

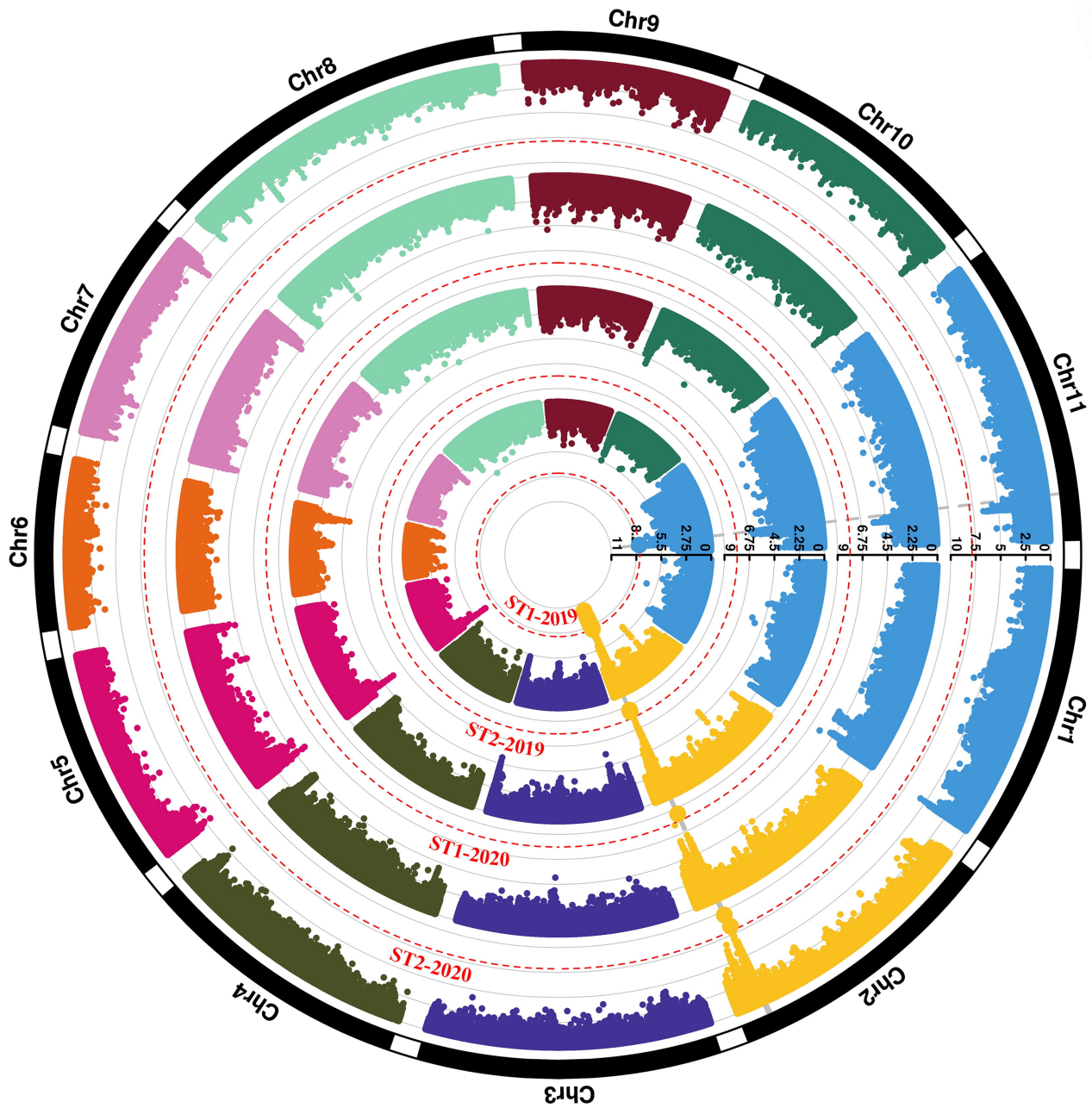


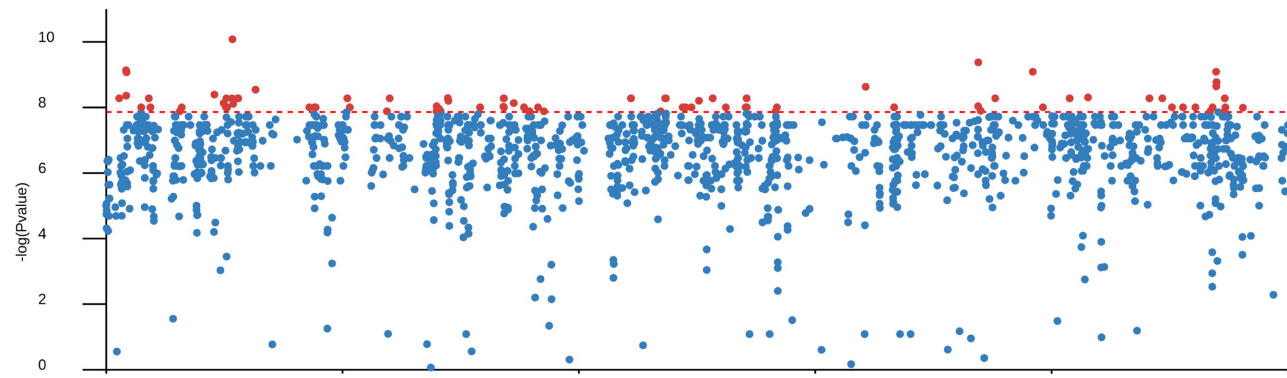
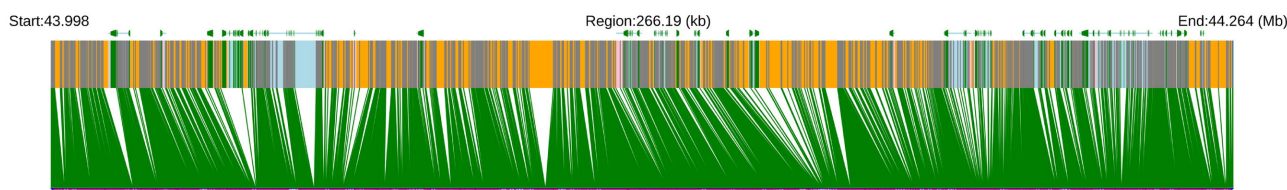
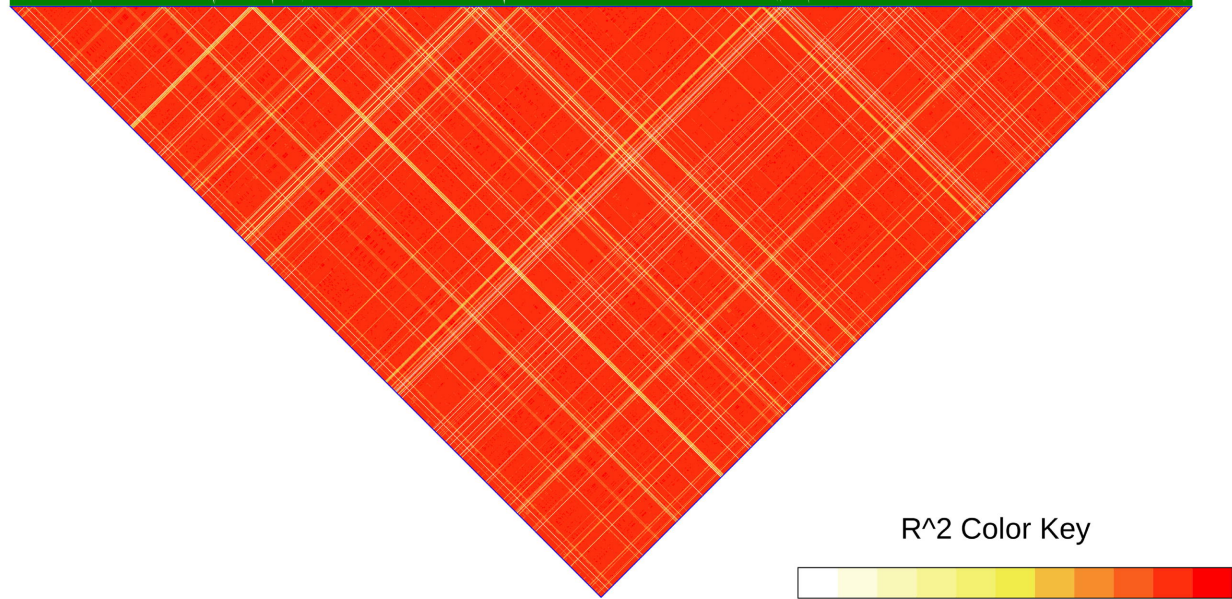
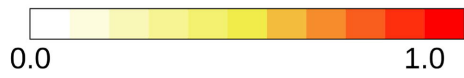
The number of SNPs within 1Mb window size

0Mb 7Mb 14Mb 21Mb 28Mb 35Mb 42Mb 49Mb 56Mb 63Mb







A**B****C****R² Color Key**

A**B**